

Universal active disturbance rejection control for non-linear systems with multiple disturbances via a high-order sliding mode observer

Chen Dai¹, Jun Yang¹✉, Zuo Wang¹, Shihua Li¹

¹School of Automation, Southeast University, Key Laboratory of Measurement and Control of Complex Systems of Engineering, Ministry of Education, Nanjing 210096, Jiangsu, People's Republic of China

✉ E-mail: j.yang84@seu.edu.cn

Abstract: This study is concerned with the output feedback control design for a class of non-linear systems subject to multiple sources of disturbances/uncertainties including parameter perturbations, complicated non-linear dynamics and external disturbances. By developing the high-order sliding mode observer, both state and disturbance observations are incorporated into the controller design. By means of the lumped disturbance estimation as well as virtual state estimations, a composite output feedback controller combined with an additional feedforward compensation is proposed. The stability of the closed-loop system is rigorously demonstrated based on Lyapunov stability criterion. Application of the proposed approach to a single-phase DC–AC inverter system is finally implemented with experimental results to validate the feasibility and effectiveness.

1 Introduction

Various disturbances and uncertainties including parameter perturbations, complicated non-linear dynamics and external disturbances widely exist in industrial systems. They often bring about adverse influences to the stability and performance of control systems. Taking the DC–AC inverter system as an example, it behaves complicated non-linear dynamics and is interfered by different sources of disturbances/uncertainties, such as load variations, parameter perturbations, electro-magnetic interference, measurement errors, actuator degradation and so on [1–4]. Those disturbances will deteriorate the control performance, such as resulting in undesirable harmonic ripples that may cause breakage or fatigue to costly machine components. Consequently, disturbance rejection and uncertainty attenuation are imperative in modern industrial control.

Up to present, a number of elegant control approaches have been investigated in the literature to handle disturbances and uncertainties, such as non-linear robust control [5, 6], sliding mode control [7–10], adaptive control [11], output regulation control [12], backstepping control [13, 14] and so on. In general, the aforementioned control methods can be classified into the following two categories. The first category mainly focuses on the stability (or robust stability) of systems via some classical control design tools, such as Riccati approach [15], adaptive approach [16] and linear matrix inequality (LMI)-based approach [17]. The second category, like integral sliding model control (I-SMC) approach [18], aims to utilise the integral action to remove the offset caused by disturbances/uncertainties. Although both of them have been proved to be efficient and been extensively applied, they handle the disturbances/uncertainties in a robust way. Owing to this, the disturbances/uncertainties are finally rejected at cost of sacrificing the nominal control performance [19, 20]. Moreover, without effective feedforward disturbance compensation, the non-vanishing disturbances could not be entirely eliminated, but only be attenuated to a certain level.

As a practical alternative approach, the active disturbance rejection control (ADRC) method is deemed to be prominent in both performance and practicality [21]. With its promising outlook and possibilities, the ADRC method has been widely applied in various industrial applications, including motor drives, manipulators, gyroscopes control systems, mechatronic systems [22–24] and so on. The concept of non-linear feedback control and

the method of total disturbance estimation/rejection are deemed as the key thoughts of the ADRC law. To estimate the disturbances precisely, several effective methods have been applied, such as the disturbance observer [25–27], the extended state observer (ESO) [28, 29], the generalised proportional–integral observer (GPIO) [30] and so on. However, each of the aforementioned methods has limitations in disturbance rejection and uncertainty attenuation. In addition, the ESOs mainly focus on slow-time varying; the GPIOs only work for polynomial disturbances, but cannot achieve asymptotic estimations for other types of disturbances. Actually, in most practical applications, there exist multiple sources of disturbances and uncertainties, such as slow-time varying disturbances, polynomial and periodic harmonic disturbances. Furthermore, most of the aforementioned observers could only achieve approximate estimations and converge within a comparatively long time interval. A natural concern is whether it is possible to develop a universal ADRC approach with a finite-time convergent observer to handle different types of disturbances/uncertainties simultaneously.

Following the above motivations, a universal ADRC (UADRC) strategy using high-order sliding mode observer (HOSMO) is developed in this paper for non-linear systems subject to multiple sources of disturbances and uncertainties, especially the model uncertainties and input variations in different forms. First, all of the disturbances and uncertainties are considered as a lumped one. An arbitrary-order finite-time-convergent exact robust observer is then constructed based on the high-order sliding mode technique [31, 32]. Subsequently, a universal extended state observer is employed to estimate both of the lumped disturbance and virtual states. A composite controller is finally developed for asymptotically offset tracking of the closed-loop system even in the presence of multiple sources of disturbances and uncertainties. The main idea of the proposed method is to integrate the output feedback control with additional feedforward compensations provided by the HOSMO. The major remarkable merits of the proposed UADRC method can be summarised as follows:

- i. The proposed UADRC method inherits the advantages of the conventional ADRC method. The concept of the lumped disturbance is introduced to estimate the unknown state and disturbances/uncertainties, which largely simplifies the control law. Actually, similar to the conventional ADRC method, only

the system order is required for the design. In other words, the presented approach can be deemed as an almost model free approach, which declines the demand for sensors to a large extent. The reduction of sensors will decrease the complexity, cost, space of the system and enhance system reliability consequently, which is of much significance to the performance of the control system [33].

- ii. The proposed UADRC method is supposed to be an enhanced version of the conventional ADRC method in the sense that it can deal with multiple sources of disturbances and uncertainties simultaneously. It provides the non-linear system with an instantaneous remedy for many different types of disturbances/uncertainties rather than single type of disturbances/uncertainties in the conventional ADRC method. In addition, the proposed controller has a simple structure, a small amount of tuning parameters and easy tuning procedures. The proposed HOSMO is finite-time convergent, providing precise estimations of both the virtual states and multiple sources of disturbances/uncertainties.

The rest of the paper is organised as follows. In Section 2, the problem formulation of this paper is introduced. In Section 3, details on the controller design are presented, followed by the rigorous stability analysis of the closed-loop system. In Section 4, a tracking control example of a DC–AC inverter system is provided with simulation and experimental studies to validate the efficiency of the proposed method. Finally, the paper is concluded in Section 5.

2 UADRC design

2.1 Problem formulation

A class of single-input single-output non-linear dynamic systems subject to multiple sources of disturbances and uncertainties is considered here, which is depicted by

$$y^{(m)}(t) = f(y(t), \dots, y^{(n-1)}(t), t) + bu(t) + d_e(t), \quad (1)$$

where $y(t) \in \mathbb{R}$ is the controlled output, $u(t) \in \mathbb{R}$ is the control input, $d_e(t) \in \mathbb{R}$ is the external disturbance, b is an unknown constant with a known sign [19, 34], and $f(y(t), \dots, y^{(n-1)}(t), t)$ denotes the unknown uncertain dynamics of the system, which is a function in terms of the system states and external disturbances.

Letting $\zeta_i(t) = y^{(i-1)}(t)$ for $i = 1, \dots, n$, the plant (1) is represented by the following multiple integrators system:

$$\begin{aligned} \dot{\zeta}_i(t) &= \zeta_{i+1}(t), \quad i = 1, \dots, n-1, \\ \dot{\zeta}_n(t) &= f(y(t), \dots, y^{(n-1)}(t), t) + bu(t) + d_e(t), \\ y(t) &= \zeta_1(t). \end{aligned} \quad (2)$$

The object here is to make the system output y track the reference output accurately in the presence of multiple sources of disturbances/uncertainties. The following coordinate transformation is utilised for the purpose of tracking control design. Define

$$\begin{aligned} x_1(t) &= \zeta_1(t) - y_r(t), \\ x_2(t) &= \zeta_2(t) - \dot{y}_r(t), \\ &\vdots \\ x_n(t) &= \zeta_n(t) - y_r^{(n-1)}(t), \end{aligned} \quad (3)$$

where $y_r(t)$ is the reference output of the system. Thus, the system (2) can be rewritten as

$$\begin{aligned} \dot{x}_i(t) &= x_{i+1}(t), \quad i = 1, \dots, n-1, \\ \dot{x}_n(t) &= b_0 u(t) + d(t), \\ y(t) &= x_1(t) + y_r(t), \end{aligned} \quad (4)$$

with

$$d(t) = f(x_1(t), \dots, x_n(t), t) + (b - b_0)u(t) + d_e(t) - y_r^{(n-1)}(t),$$

where $x = [x_1, \dots, x_n]^T \in \mathbb{R}^n$ is the state vector and b_0 is the nominal value of b . Similar to most of existing ADRC approaches, e.g. [19, 34], it is supposed that b and b_0 have the same sign. It is noticed that the disturbances and uncertainties from multiple sources are denoted as the lumped disturbance $d(t)$, consisting of the external disturbance $d_e(t)$ and the internal ones caused by model uncertainties.

2.2 Controller development

To estimate the lumped disturbance and the virtual states, a universal extended state observer using high-order sliding mode [10, 31, 35] is applied to system (4), given by (see (5)), where $\lambda_i > 0 (i = 1, \dots, n+1)$ are coefficients of the observer to be designed, and $z_i (i = 1, \dots, n+1)$ are the real-time robust estimations of $x_i (i = 1, \dots, n)$ and d , respectively, i.e. $\hat{x}_1 = z_1, \hat{x}_2 = z_2, \dots, \hat{x}_n = z_n, \hat{d} = z_{n+1}$. Suppose that \dot{d} is bounded by a constant K .

To drive the system output to the desired equilibrium point asymptotically, estimations of the lumped disturbance and virtual states are incorporated in the output feedback control method. The UADRC law is designed as

$$u = -b_0^{-1}(c_1 x_1 + c_2 \hat{x}_2 + \dots + c_n \hat{x}_n + \hat{d}), \quad (6)$$

where $c_i > 0 (i = 1, \dots, n)$ are the parameters to be designed.

3 Stability analysis

In this section, the stability of the closed-loop system is analysed in detail. The following assumption and lemma are firstly presented as a significant preliminary.

Assumption 1 ([31, 35]): The disturbance $d(t)$ is first-order differentiable and its derivative $\dot{d}(t)$ is bounded by a constant K .

$$\begin{aligned} \dot{z}_1 &= v_1, \quad v_1 = -\lambda_1 K^{1/(n+1)} |z_1 - x_1|^{(n/(n+1))} \text{sign}(|z_1 - x_1|) + z_2, \\ \dot{z}_2 &= v_2, \quad v_2 = -\lambda_2 K^{1/n} |z_2 - v_1|^{(n-1)/n} \text{sign}(|z_2 - v_1|) + z_3, \\ &\vdots \\ \dot{z}_i &= v_i, \quad v_i = -\lambda_i K^{1/(n+2-i)} |z_i - v_{i-1}|^{(n+1-i)/(n+2-i)} \text{sign}(z_i - v_{i-1}) + z_{i+1}, \\ &\vdots \\ \dot{z}_n &= v_n + b_0 u, \quad v_n = -\lambda_n K^{1/2} |z_n - v_{n-1}|^{1/2} \text{sign}(z_n - v_{n-1}) + z_{n+1}, \\ \dot{z}_{n+1} &= v_{n+1}, \quad v_{n+1} = -\lambda_{n+1} K \text{sign}(z_{n+1} - v_n), \end{aligned} \quad (5)$$

Lemma 1 ([36]): Consider a non-linear system $\dot{x} = F(x, u)$, which is input-to-state stable. If the input satisfies $\lim_{t \rightarrow \infty} u(t) = 0$, then the state $\lim_{t \rightarrow \infty} x(t) = 0$.

The stability of the closed-loop system is analysed here based on the Lyapunov stability method.

Theorem 1: Suppose that Assumption 1 is satisfied for system (4). Under the proposed UADRC law (6), the output y of system (4) will converge to the desired reference y_r asymptotically, if the control parameters $c_i (i = 1, \dots, n)$ are chosen appropriately so that the polynomial $p(s) = s^n + c_n s^{n-1} + \dots + c_2 s + c_1 = 0$ is Hurwitz.

Proof: Step 1: Finite-time convergence of the observer

For system (4), the estimation errors are defined as

$$e_1 = \hat{x}_1 - x_1, \quad e_2 = \hat{x}_2 - x_2, \dots, e_n = \hat{x}_n - x_n, \quad e_{n+1} = \hat{d} - d \quad (7)$$

Taking derivative of (7) and combining with (4) and (5), the observer error dynamics are depicted as (see (8)). Since $|d| \leq K$, we have

$$\dot{e}_{n+1} \in -\lambda_{n+1} K \text{sign}(z_{n+1} - v_n) + [-K, K]. \quad (9)$$

Notice that

$$z_i - v_{i-1} = (z_i - x_i) - (v_{i-1} - x_i) = e_i - \dot{e}_{i-1}, \quad i = 2, \dots, n \quad (10)$$

is used here to derive the formula in (8).

Denoting $\sigma_i = e_i/K, i = 1, \dots, n+1$, one obtains

$$\begin{aligned} \dot{\sigma}_1 &= -\lambda_1 |\sigma_1|^{n/(n+1)} \text{sign}(\sigma_1) + \sigma_2, \\ \dot{\sigma}_i &= -\lambda_i |\sigma_i - \dot{\sigma}_{i-1}|^{(n+1-i)/(n+2-i)} \text{sign}(\sigma_i - \dot{\sigma}_{i-1}) + \sigma_{i+1}, \quad i = 2, \dots, n, \\ \dot{\sigma}_{n+1} &\in -\lambda_{n+1} \text{sign}(z_{n+1} - v_n) + [-1, 1]. \end{aligned} \quad (11)$$

It follows from [31] that the error system (11) is finite-time stable [5, 37], i.e. there exists a time constant $t_f > t_0$ such that $e_i(t) = 0 (i = 1, \dots, n+1)$ for $t \geq t_f$.

The dynamics of states $\hat{x}_i (i = 1, \dots, n)$ are obtained from (4) and (7), governed by

$$\begin{aligned} \dot{\hat{x}}_i &= \hat{x}_{i+1} - e_{i+1} + \dot{e}_i, \quad i = 1, \dots, n-1 \\ \dot{\hat{x}}_n &= b_0 u + d - e_{n+1} + \dot{e}_n. \end{aligned} \quad (12)$$

The dynamics (12) imply that the states suffer from the observer error dynamics (8). Next we will show that the observer error dynamics (8) will not drive the states (12) to infinity in finite time.

Step 2: Finite-time boundedness of the states

Define a finite-time bounded function $V(x_1, \hat{x}, \hat{d}) = (1/2)x_1^2 + \sum_{i=2}^n (1/2)\hat{x}_i^2 + (1/2)\hat{d}^2$ for system (12) [37]. It is useful to learn that the parameters $\alpha_i = ((n+1-i)/(n+2-i)) (i = 1, \dots, n)$ satisfy the condition that $\alpha_i \in (0, 1)$, which implies that $|e_i - \dot{e}_{i-1}|^{\alpha_i} < 1 + |e_i - \dot{e}_{i-1}|$. Taking derivative of $V(x_1, \hat{x}, \hat{d})$ along system dynamics (12), one obtains (see (13)), where $K_v = 2 + \sum_{i=1}^n c_i + (1+K)\sum_{i=2}^{n+1} \lambda_i$, and $L_v = (1/2) \max [e_2^2 + (1+K)\sum_{i=2}^n \lambda_i(e_i^2 + \dot{e}_{i-1}^2)]$.

It is shown from (8) that the derivatives of the estimation errors \dot{e}_i are bounded and that the estimation errors e_i have been proved to converge to zero in finite time, which guarantees that $e_i (i = 1, \dots, n+1)$ and so L_v are bounded. Therefore, it can be concluded from (7) and (13) that $V(x_1, \hat{x}, \hat{d})$ and so the states \hat{x}_i and $x_i (i = 1, \dots, n)$ will not escape to infinity before the finite-time convergence of observer error dynamics [37].

Step 3: Asymptotical convergence of the tracking error

Combining (4) with (7), \dot{x}_n can be written as

$$\begin{aligned} \dot{x}_n &= b_0 u + d \\ &= -(c_1 x_1 + c_2 x_2 + \dots + c_n x_n) - (\hat{d} - d) \\ &= -(c_1 x_1 + c_2 x_2 + \dots + c_n x_n + c_2 e_2 + \dots + c_n e_n) - e_{n+1}. \end{aligned} \quad (14)$$

Once the finite-time stability of (11) is achieved, i.e. $e_i = 0 (i = 1, \dots, n+1)$, (14) will reduce to

$$\dot{x}_n = -(c_1 x_1 + c_2 x_2 + \dots + c_n x_n), \quad (15)$$

thus the system dynamics (4) will reduce to the following compact form:

$$\dot{x} = Ax, \quad (16)$$

where $x = [x_1, \dots, x_n]^T$, and

$$A = \begin{bmatrix} 0 & 1 & \cdots & 0 \\ \vdots & \vdots & \ddots & \vdots \\ 0 & 0 & \cdots & 1 \\ -c_1 & -c_2 & \cdots & -c_n \end{bmatrix}$$

with $c_i > 0 (i = 1, \dots, n)$.

When the parameters $c_i (i = 1, \dots, n)$ is chosen such that the polynomial $p(s) = s^n + c_n s^{n-1} + \dots + c_2 s + c_1 = 0$ is Hurwitz, then the matrix A is Hurwitz. Consequently, the closed-loop system (4) is asymptotically stable. We have

$$\lim_{t \rightarrow \infty} x_1(t) = 0, \quad (17)$$

that is

$$\lim_{t \rightarrow \infty} y(t) = y_r(t). \quad (18)$$

This completes the proof. \square

Remark 1: The rationality and effectiveness of Assumption 1 can be referred to [31, 35]. Actually, many practical disturbances including constant, sinusoidal and any bounded smooth disturbances satisfy the condition given in Assumption 1.

4 Application to a DC–AC inverter system

Nowadays, power electronics are playing a propelling role in industrial automation, transportation, city power, energy saving, environment pollution control and so on. As one of the most significant parts of power electronics, the DC–AC inverter is widely utilised to realise the conversion of DC power to AC power. Accordingly, DC–AC inverter technology has been extensively employed in various industrial applications such as hybrid electric

$$\begin{aligned} \dot{e}_1 &= -\lambda_1 K^{1/(n+1)} |e_1|^{n/(n+1)} \text{sign}(e_1) + e_2, \\ \dot{e}_i &= -\lambda_i K^{1/(n+2-i)} |e_i - \dot{e}_{i-1}|^{(n+1-i)/(n+2-i)} \text{sign}(e_i - \dot{e}_{i-1}) + e_{i+1}, \quad i = 2, \dots, n, \\ \dot{e}_{n+1} &= -\lambda_{n+1} K \text{sign}(z_{n+1} - v_n) - \dot{d}. \end{aligned} \quad (8)$$

$$\begin{aligned}
\dot{V} &= x_1 \dot{x}_1 + \sum_{i=2}^n \hat{x}_i \dot{\hat{x}}_i + \dot{\hat{d}} \dot{\hat{d}} \\
&= x_1 (\hat{x}_2 - e_2) + \sum_{i=2}^{n-1} \hat{x}_i v_i + \hat{x}_n (v_n + b_0 u) + \dot{\hat{d}} v_{n+1} \\
&= x_1 (\hat{x}_2 - e_2) + \sum_{i=2}^n \hat{x}_i v_i + \hat{x}_n b_0 u + \dot{\hat{d}} v_{n+1} \\
&= x_1 (\hat{x}_2 - e_2) + \sum_{i=2}^n \hat{x}_i [-\lambda_i K^{1-\alpha_i} |e_i - \dot{e}_{i-1}|^{\alpha_i} \text{sign}(e_i - \dot{e}_{i-1}) + \hat{x}_{i+1}] \\
&\quad - \hat{x}_n (c_1 x_1 + \sum_{i=2}^n c_i \hat{x}_i) + \dot{\hat{d}} [-\lambda_{n+1} K \text{sign}(e_n - \dot{e}_{n-1})] \\
&\leq x_1 \hat{x}_2 - x_1 e_2 + \sum_{i=2}^n \hat{x}_i [-\lambda_i (1+K)(1+|e_i - \dot{e}_{i-1}|) + \hat{x}_{i+1}] \\
&\quad - c_1 \hat{x}_n x_1 - \hat{x}_n \sum_{i=2}^n c_i \hat{x}_i + \lambda_{n+1} K |\dot{\hat{d}}| \\
&\leq |x_1 \hat{x}_2| + |x_1 e_2| + \sum_{i=2}^{n-1} |\hat{x}_i \hat{x}_{i+1}| + |\hat{x}_n \dot{\hat{d}}| + c_1 |\hat{x}_n x_1| + \sum_{i=2}^n c_i |\hat{x}_n \hat{x}_i| \\
&\quad + (1+K) \sum_{i=2}^n \lambda_i |\hat{x}_i| (1+|e_i - \dot{e}_{i-1}|) + \lambda_{n+1} K |\dot{\hat{d}}| \\
&\leq \frac{x_1^2 + \hat{x}_2^2}{2} + \frac{x_1^2 + e_2^2}{2} + \sum_{i=2}^{n-1} \frac{\hat{x}_i^2 + \hat{x}_{i+1}^2}{2} + \frac{x_n^2 + \dot{\hat{d}}^2}{2} + c_1 \frac{\hat{x}_n^2 + x_1^2}{2} + \sum_{i=2}^n c_i \frac{\hat{x}_n^2 + \hat{x}_i^2}{2} \\
&\quad + (1+K) \sum_{i=2}^n \lambda_i \left(\frac{\hat{x}_i^2}{2} + \frac{\hat{x}_i^2 + e_i^2}{2} + \frac{\hat{x}_i^2 + e_{i-1}^2}{2} \right) + \lambda_{n+1} K \frac{\dot{\hat{d}}^2}{2} \\
&\leq K_v V + L_v
\end{aligned} \tag{13}$$

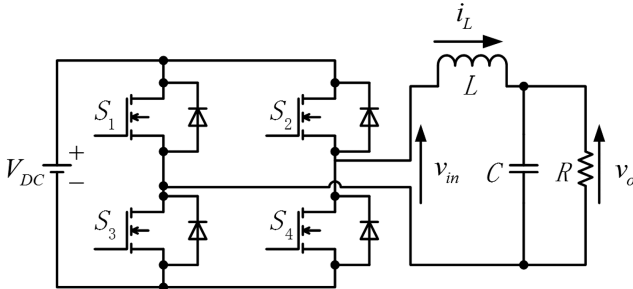


Fig. 1 Diagram of single-phase DC-AC inverter circuit

vehicles [33], inverter power [38], uninterruptible power supplies [39], active power filters [40] and so on.

As is well known, fast response, high reliability, small steady-state error and strong robustness are required for high-performance AC power supplies [41]. However, as is mentioned above, there exist different sources of disturbances/uncertainties in the practical DC-AC inverter system, such as load variations, parameter perturbations, electro-magnetic interference, measurement errors and so on. As a result, a delicate controller is imperative to achieve high dynamic and static performances.

In this section, a single-phase DC-AC inverter system is taken into consideration. The dynamic model of the system is firstly given, followed by the detailed controller design. Then, both of the simulation and experimental studies are carried out and the effectiveness and superiority of the proposed control method are finally verified.

4.1 Dynamic model of the DC-AC inverter system

The typical circuit diagram of the single-phase DC-AC inverter is shown in Fig. 1, where V_{DC} is the input direct voltage, v_{in} is the output voltage of the inverter in an sinusoidal pulse width

modulation (SPWM) waveform, $S_1 - S_4$ are switching devices, i_L is the current of the inductor, v_o is the output voltage of the capacitor, R is the resistive load of the whole circuit, L and C are the inductor and capacitor, respectively.

Using the state-space averaging method and the Kirchhoff's voltage and current laws [40, 42], the model equation can be formulated as

$$\begin{aligned}
\frac{di_L}{dt} &= \frac{uV_{DC}}{L} - \frac{v_o}{L}, \\
\frac{dv_o}{dt} &= \frac{i_L}{C} - \frac{v_o}{RC}.
\end{aligned} \tag{19}$$

Define $x_1 = e = v_{ref} - v_o$ and $x_2 = \dot{x}_1$, where v_{ref} denotes the periodic reference signal, the dynamic model of the DC-AC inverter system can be expressed as

$$\begin{aligned}
\dot{x}_1(t) &= x_2(t), \\
\dot{x}_2(t) &= b_0 u(t) + d(t), \\
y(t) &= x_1(t),
\end{aligned} \tag{20}$$

where

$$\begin{aligned}
b_0 &= -\frac{V_{DC0}}{LC}, \\
d(t) &= -\frac{1}{LC}x_1(t) - \frac{1}{RC}x_2(t) + \frac{v_{ref}}{LC} + \frac{\dot{v}_{ref}}{RC} + \ddot{v}_{ref} - \frac{\Delta V_{DC}}{LC}u.
\end{aligned} \tag{21}$$

4.2 Controller design

According to the design procedure in Section 3, the proposed UADRC method is applied here, combined with a HOSMO, given by

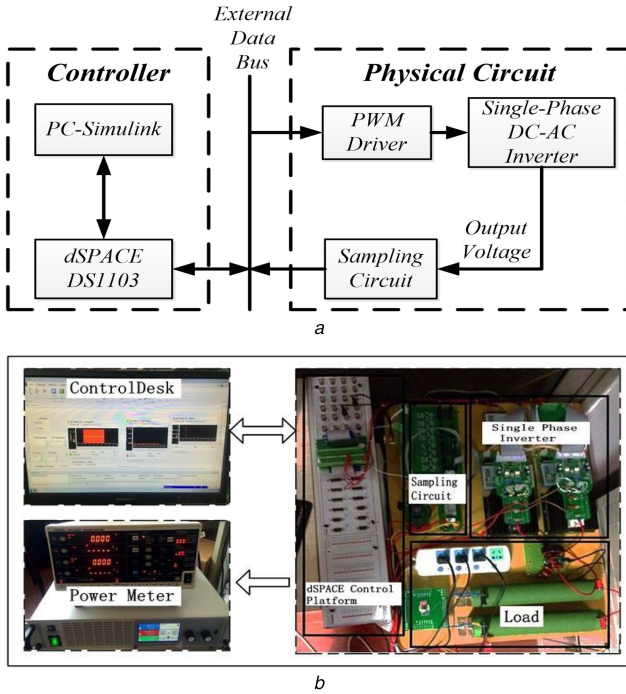


Fig. 2 Experimental test setup and the photograph of the experimental prototype
(a) Configuration of experimental setup, (b) Photograph of the experimental prototype

$$\begin{aligned}\dot{z}_1 &= v_1, \quad \dot{z}_2 = v_2 + b_0 u, \quad \dot{z}_3 = v_3, \\ v_1 &= -\lambda_1 K^{1/3} |z_1 - x_1|^{2/3} \text{sign}(z_1 - x_1) + z_2, \\ v_2 &= -\lambda_2 K^{1/2} |z_2 - v_1|^{1/2} \text{sign}(z_2 - v_1) + z_3, \\ v_3 &= -\lambda_3 K \text{sign}(z_3 - v_2),\end{aligned}\quad (22)$$

where $\lambda_i > 0 (i = 1, 2, 3)$ are coefficients of the observer to be designed, and z_2, z_3 are real-time robust estimations of x_2 and d , i.e. $\hat{x}_2 = z_2, \hat{d} = z_3$. Thus, the UADRC law is designed as

$$u = -b_0^{-1}(c_1 x_1 + c_2 \hat{x}_2 + \hat{d}), \quad (23)$$

where $c_i > 0 (i = 1, 2)$ are the parameters to be designed.

4.3 Simulation and experimental results

In this part, the robustness performance of the proposed approach against multiple sources of disturbances/uncertainties is validated by detailed simulation and experimental studies. The physical meanings and nominal values of the parameters for the DC–AC inverter system are listed in Table 1.

The DC–AC inverter system is simulated using MATLAB/Simulink tools and the experimental test setup is built based on the dSPACE DS1103 real-time control systems. The configuration of the experimental test setup and the photograph of the experimental prototype are shown in Fig. 2, respectively. Moreover, in the experimental study, the type of IGBTs is FF200R33KF2C and the switching frequency is chosen as 12 kHz. The sampling periods of three control methods are all set to be 0.1 ms.

In this part, five cases of different disturbances/uncertainties are taken into consideration, which are listed in Table 2.

To verify the efficiency of the proposed UADRC method, a conventional ADRC approach [21] and a traditional proportional–integral–derivative (PID) method are employed for comparison. The ESO of the conventional ADRC approach is designed as

$$\begin{aligned}\dot{z}_1 &= z_2 - \beta_1(z_1 - y), \\ \dot{z}_2 &= b_0 u + z_3 - \beta_2(z_1 - y), \\ \dot{z}_3 &= -\beta_3(z_1 - y),\end{aligned}\quad (24)$$

Table 1 Parameters of the DC–AC inverter

Parameters	Meanings	Nominal values
V_{DC0}	input voltage	50 V
v_{ref}	reference output voltage	$30\cos(100\pi t)$ V
L	inductance	1×10^{-3} H
C	capacitance	5.25×10^{-6} F
R	load resistance	100Ω

Table 2 Simulation and experimental cases

Cases	Disturbances	Uncertainties
1	none	input voltage variation: $V_{DC} = 50V \rightarrow 35V$
2	none	load variation: $R = 100\Omega \rightarrow 50\Omega$
3	step form input: $d_u(t) = 0.1, t \geq 0.01s$	nominal load: $R = 100\Omega$
4	sawtooth form input: $d_u(t) = \frac{0.1}{T}(t - KT), KT < t < (K + 1)T$	nominal load: $R = 100\Omega$
5	sinusoidal form input: $d_u(t) = 0.1\sin(500\pi t)$	nominal load: $R = 100\Omega$

Table 3 Control parameters for the DC–AC inverter system
Controllers Parameters

UADRC	$c_1 = 0.084, c_2 = 4.2 \times 10^{-6}, K = 2.5 \times 10^7, \lambda_1 = 2, \lambda_2 = 1.5, \lambda_3 = 1.1$
ADRC	$\beta_1 = 1.575 \times 10^{-6}, \beta_2 = 0.0144, \beta_3 = 39.375, k_1 = 9 \times 10^8, k_2 = 60,000$
PID	$k_P = 4.8 \times 10^7, k_I = 6.4 \times 10^{10}, k_D = 12000$

where z_2, z_3 are the estimates of the system state x_2 and the lumped disturbance d , respectively. The conventional ADRC law is designed as

$$u = -b_0^{-1}(k_1 x_1 + k_2 z_2 + z_3). \quad (25)$$

The corresponding PID law is designed as

$$u = -b_0^{-1}(k_P x_1 + k_I \int_0^t x_1(\tau) d\tau + k_D \dot{x}_1). \quad (26)$$

To have a fair comparison, the amplitudes of control signal of the three controllers are kept at the same level, and proper control parameters are carefully chosen for them, which are listed in Table 3.

Case 1: Tests in the presence of input voltage variation: In this case, the direct input voltage V_{DC} changes from its nominal value $V_{DC} = V_{DC0} = 50$ V to $V_{DC} = 35$ V at $t = 0.025$ s. The simulation and experimental results are shown in Figs. 3 and 4, respectively. As is shown in Fig. 3, the undesirable effect of the input voltage variation can be quickly eliminated by the proposed UADRC method, accompanied with the smallest tracking error as well. The experimental results in Fig. 4 have also validated the best control characteristics of the proposed UADRC method compared with the PID and ADRC methods.

Case 2: Tests in the presence of load variations: In this case, the load resistance changes from its nominal value $R = R_0 = 100\Omega$ to $R = 50\Omega$ at $t = 0.02$ s. The simulation and experimental results are shown in Figs. 5 and 6, respectively. As is shown in Figs. 5 and 6, the duty ratio amplitudes are kept at the same level for the three control methods. It is observed from Figs. 5e and f that the HOSMO has a higher estimation precision and stronger antijamming feature than those of the ESO. As such, both of the

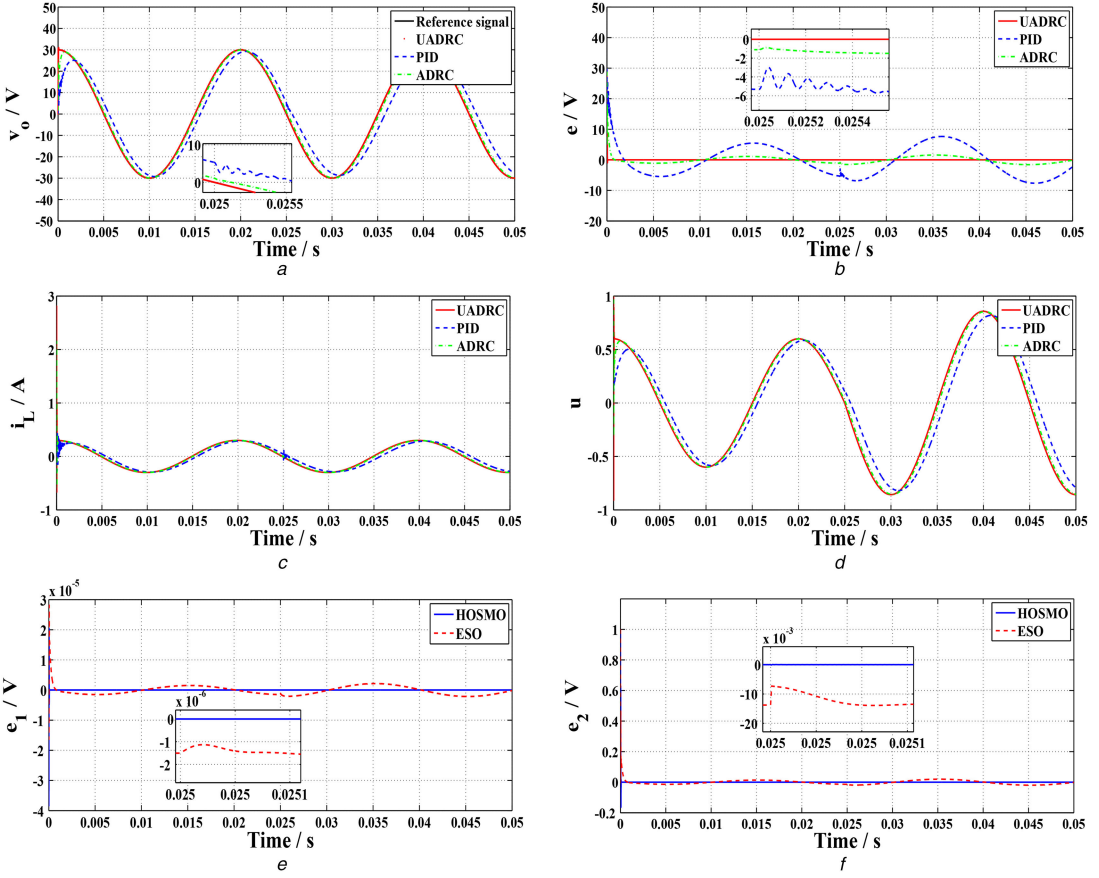


Fig. 3 System performances in the presence of input voltage variation

(a) output voltage, (b) tracking errors, (c) inductance current, (d) duty ratio, (e) estimating error of x_2 , (f) estimating error of lumped disturbance. (Case 1: Simulation results)

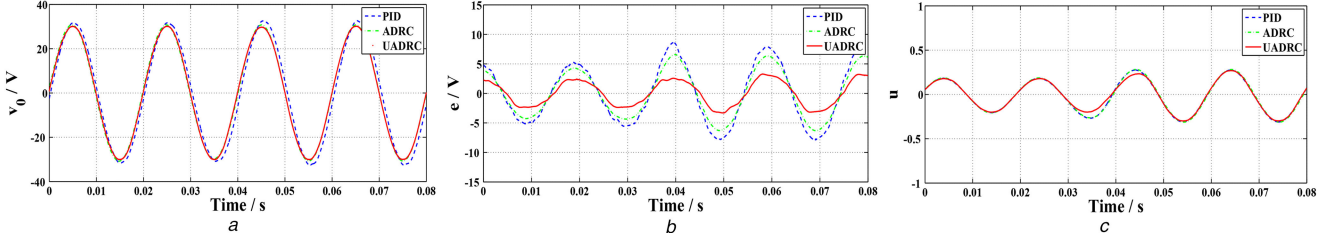


Fig. 4 System performances in the presence of input voltage variation

(a) Output voltage v_o , (b) Tracking errors e , (c) Duty ratio u (Case 1: experimental results)

simulation and experimental results validate that the proposed UADRC method exhibits a much smaller tracking error than those of the PID and ADRC methods and can ultimately attenuate the load variations.

Case 3: Tests in the presence of step form input disturbance: In this case, a step form disturbance is imposed on the system via the input channel, which can be expressed as

$$d_u(t) = \begin{cases} 0 & 0 \leq t < 0.01 \text{ s}, \\ 0.1 & t \geq 0.01 \text{ s}. \end{cases} \quad (27)$$

System responses in the simulation and experimental tests are presented in Figs. 7 and 8, respectively.

It is clearly shown in Figs. 7 and 8 that the proposed UADRC method can track the reference voltage more accurately after the step input and there are relatively larger tracking errors for the PID and ADRC methods. In addition, Figs. 7e and f show that the HOSMO has better estimation precision and robustness than the ESO. According to the simulation and experimental results, it turns out that the proposed UADRC method can ultimately attenuate the step form input disturbance.

Case 4: Tests in the presence of sawtooth form input disturbance: In this case, a sawtooth form disturbance is imposed on the system via the input channel, which can be expressed as

$$d_u(t) = \begin{cases} 0 & t = KT, \\ \frac{A}{T}(t - KT) & KT < t < (K + 1)T, \quad K = 0, 1, 2, \dots \end{cases} \quad (28)$$

where $A = 0.1 \text{ V}$, $T = 0.004 \text{ s}$.

Simulation and experimental results are presented in Figs. 9 and 10, respectively. It is shown in Figs. 9 and 10 that there exist serious ripples in sawtooth form under control of the PID method, which indicates that the PID method fails to achieve robustness against the given disturbance. Although the conventional ADRC method can basically attenuate the given disturbance, the amplitude of the ripples is averagely larger than the proposed method. In addition, it is shown in Figs. 9e and f that the estimating performance of the HOSMO is of a higher precision so that it can provide an accurate estimate for the UADRC law to compensate the disturbance. Both of the simulation and experimental results verify that the proposed UADRC method exhibits better robustness and control performance than other two methods.

Case 5: Tests in the presence of sinusoidal form input disturbance: In this case, a sinusoidal form disturbance is imposed on the system via the input channel, which can be expressed as

$$d_u(t) = 0.1 \sin(500\pi t). \quad (29)$$

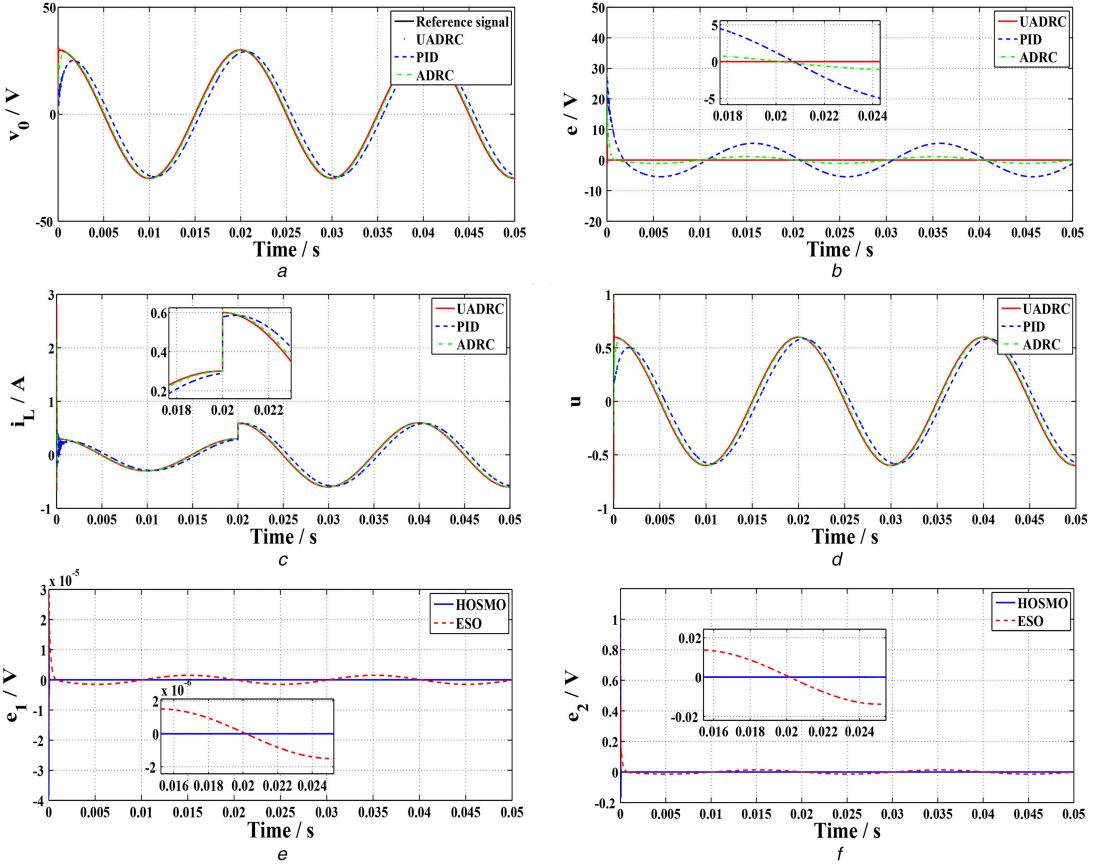


Fig. 5 System performances in the presence of input voltage variation

(a) output voltage, (b) tracking errors, (c) inductance current, (d) duty ratio, (e) estimating error of x_2 , (f) estimating error of lumped disturbance. (Case 2: Simulation results)

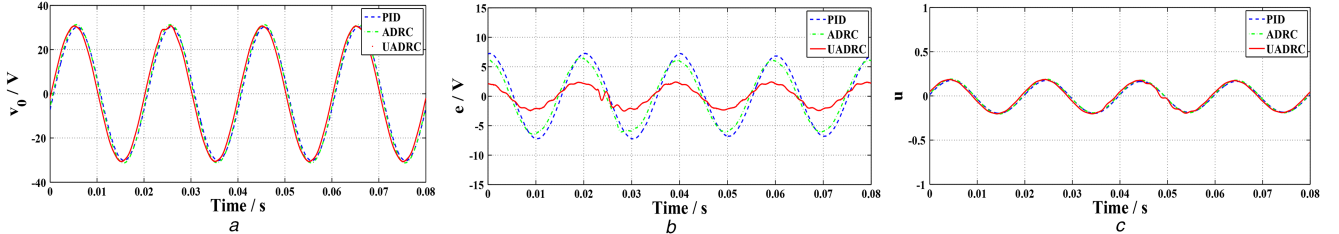


Fig. 6 System performances in the presence of load variations

(a) Output voltage v_o , (b) Tracking errors e , (c) Duty ratio u (Case 2: experimental results)

System responses yielded by all the three methods and observer estimations are presented and compared in Figs. 11 and 12, respectively.

As shown in Figs. 11 and 12, the PID and ADRC methods result in more serious chattering phenomenon in the presence of the imposed disturbance, while the UADRC method still achieves satisfactory dynamic and static performance with strong robustness against the sinusoidal form input disturbance. Furthermore, it is observed from Figs. 11e and f that the HOSMO has smaller fluctuations and can recover and converge to zero again more rapidly than the ESO. Consequently, the proposed method achieves better disturbance rejection ability as well as tracking accuracy.

To sum up, in the five cases above, the proposed UADRC method achieves more satisfactory dynamic/static performance and stronger antijamming capability compared with the PID and ADRC methods.

5 Conclusions

In this paper, a universal active disturbance rejection control using high-order sliding mode observer has been proposed for a class of non-linear systems to attenuate multiple sources of disturbances/uncertainties including load variations, input disturbances in the step, sawtooth and sinusoidal forms and so on. By means of the estimation and compensation of the lumped disturbance and virtual

states, a composite output feedback controller has been developed for multiple disturbances/uncertainties rejection. To validate the effectiveness and feasibility of the proposed method, application to a single-phase DC–AC inverter system is investigated with detailed simulation and experimental studies in comparison with the PID and the conventional ADRC method. The simulation and experimental results have validated the robustness and control performance of the proposed method.

6 Acknowledgments

This work was supported in part by National Natural Science Foundation of China under grants 61203011, 61473080 and 61403227, PhD Program Foundation of Ministry of Education of China under Grant 20120092120031, and Natural Science Foundation of Jiangsu Province under Grant BK2012327.

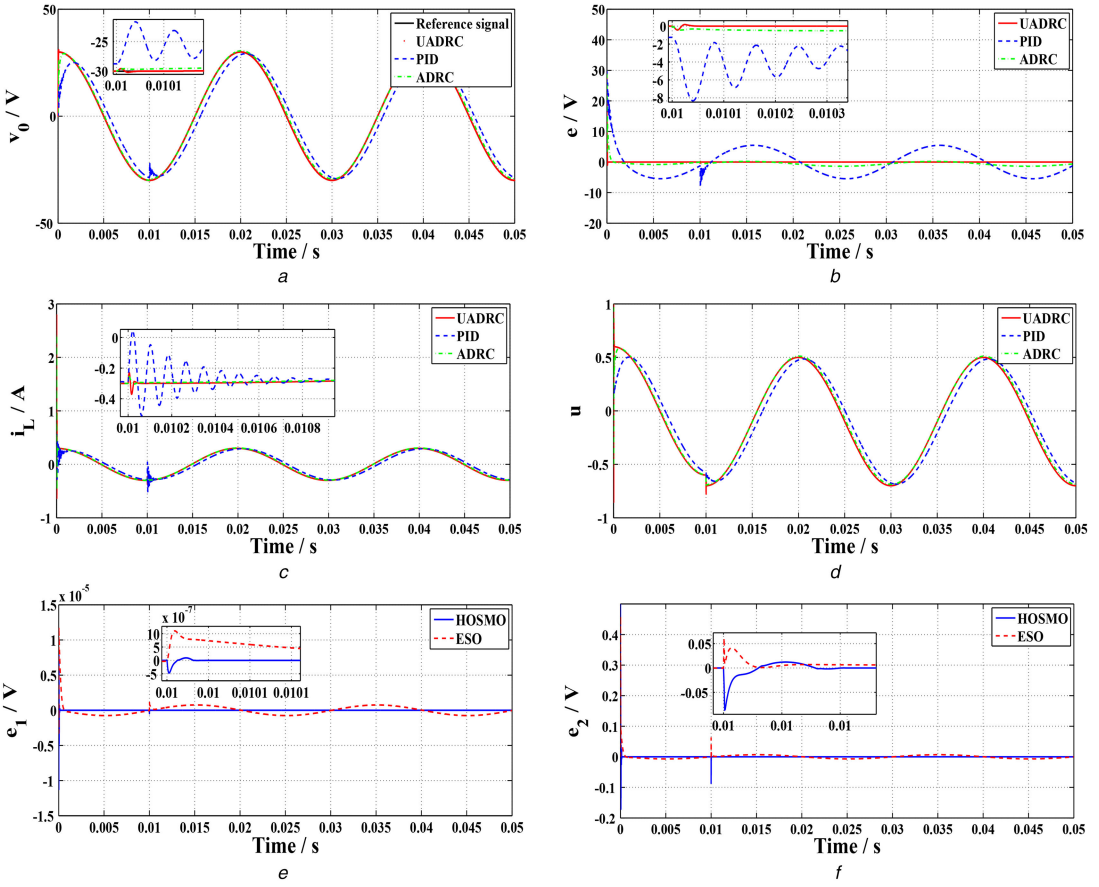


Fig. 7 System performances in the presence of input voltage variation

(a) output voltage, (b) tracking errors, (c) inductance current, (d) duty ratio, (e) estimating error of x_2 , (f) estimating error of lumped disturbance. (Case 3: Simulation results)

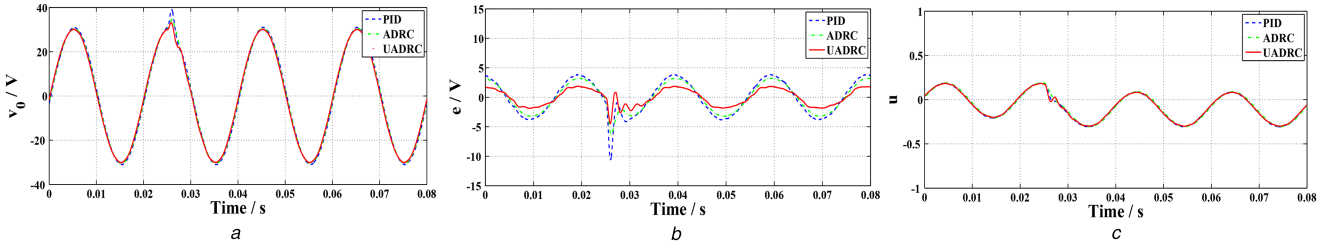


Fig. 8 System performances in the presence of step form input disturbance

(a) Output voltage v_o , (b) Tracking errors e , (c) Duty ratio u (Case 3: experimental results)

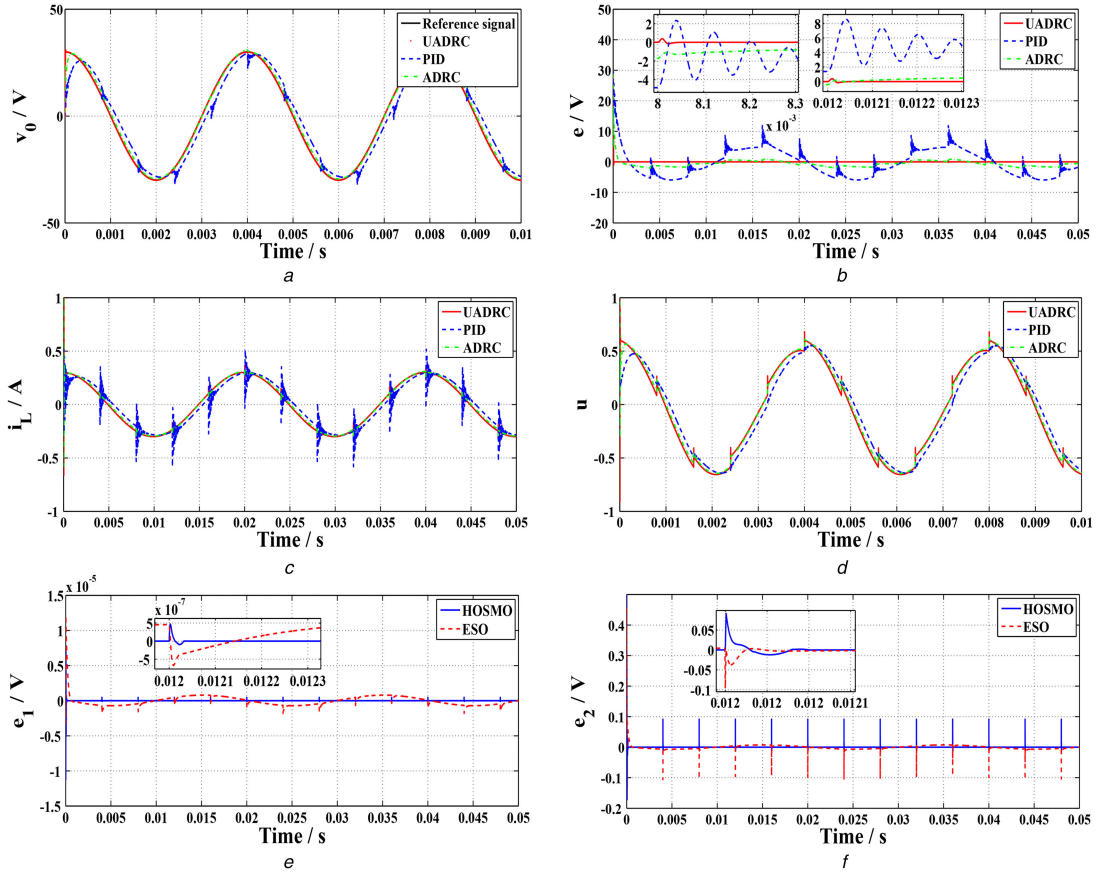


Fig. 9 System performances in the presence of input voltage variation

(a) output voltage, (b) tracking errors, (c) inductance current, (d) duty ratio, (e) estimating error of x_2 , (f) estimating error of lumped disturbance. (Case 4: Simulation results)

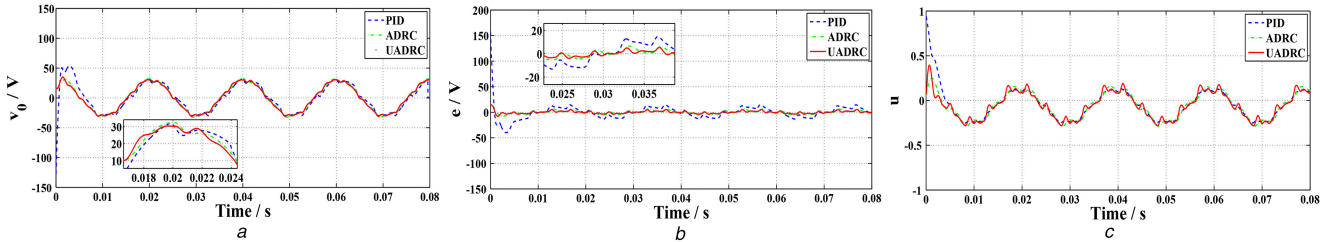


Fig. 10 System performances in the presence of sawtooth form input disturbance

(a) Output voltage v_o , (b) Tracking errors e , (c) Duty ratio u (Case 4: experimental results)

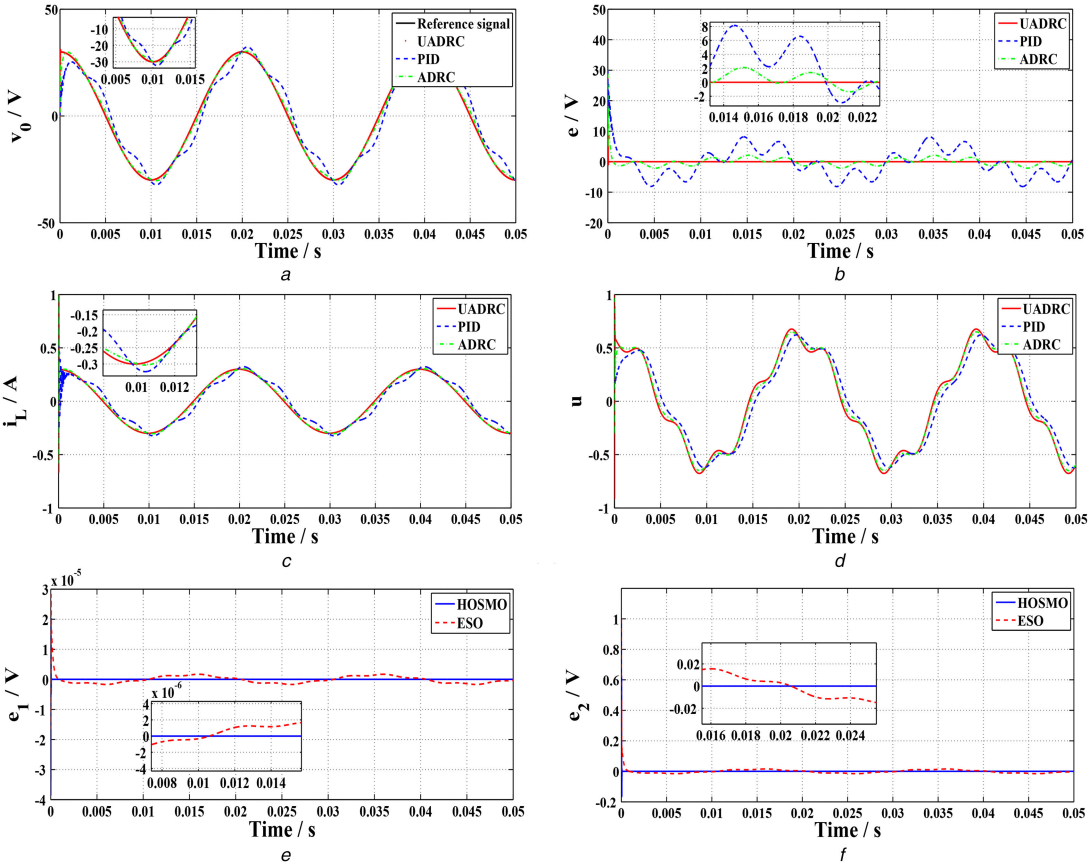


Fig. 11 System performances in the presence of input voltage variation

(a) output voltage, (b) tracking errors, (c) inductance current, (d) duty ratio, (e) estimating error of x_2 , (f) estimating error of lumped disturbance. (Case 5: Simulation results)

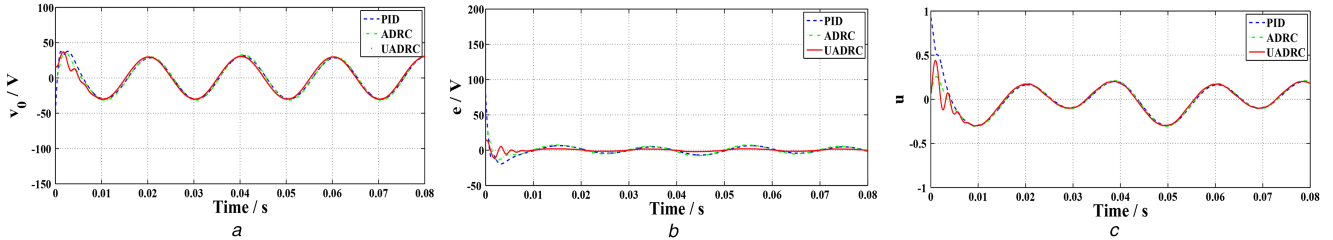


Fig. 12 System performances in the presence of sinusoidal form input disturbance

(a) Output voltage v_o , (b) Tracking errors e , (c) Duty ratio u (Case 5: experimental results)

7 References

- [1] Lu, W.Z., Zhou, K.L., Wang, D.W., et al.: ‘A general parallel structure repetitive control scheme for multiphase DC–AC PWM converters’, *IEEE Trans. Power Electron.*, 2013, **28**, (8), pp. 3980–3987
- [2] Ye, Y.Q., Zhou, K.L., Zhang, B., et al.: ‘High-performance repetitive control of PWM DC–AC converters with real-time phase-lead FIR filter’, *IEEE Trans. Circuit Syst.*, 2006, **16**, (6), pp. 768–772
- [3] Chen, B., Niu, Y.G., Zou, Y.Y.: ‘Adaptive sliding mode control for stochastic Markovian jumping systems with actuator degradation’, *Automatica*, 2013, **49**, (6), pp. 1748–1754
- [4] Liu, J.X., Laghrouche, S., Harmouche, M., et al.: ‘Adaptive-gain second-order sliding mode observer design for switching power converters’, *Control Eng. Pract.*, 2014, **30**, pp. 124–131
- [5] Khoo, S.Y., Xie, L.H., Man, Z.H.: ‘Robust finite-time consensus tracking algorithm for multirobot systems’, *IEEE/ASME Trans. Mechatron.*, 2009, **14**, (2), pp. 219–228
- [6] Yang, S., Lei, Q., Peng, F.Z., et al.: ‘A robust control scheme for grid-connected voltage-source inverters’, *IEEE Trans. Ind. Electron.*, 2011, **58**, (1), pp. 202–212
- [7] Song, J., Niu, Y.G., Zou, Y.Y.: ‘Finite-time sliding mode control synthesis under explicit output constraint’, *Automatica*, 2016, **65**, pp. 111–114
- [8] Wu, L.G., Zheng, W.X., Gao, H.J.: ‘Dissipativity-based sliding mode control of switched stochastic systems’, *IEEE Trans. Autom. Control*, 2013, **58**, (3), pp. 785–791
- [9] Ding, S.H., Wang, J., Zheng, W.X.: ‘Second-order sliding mode control for nonlinear uncertain systems bounded by positive functions’, *IEEE Trans. Ind. Electron.*, 2015, **62**, (9), pp. 5899–5909
- [10] Liu, J.X., Luo, W.S., Yang, X.Z., et al.: ‘Robust model-based fault diagnosis for PEM fuel cell air-feed system’, *IEEE Trans. Ind. Electron.*, 2016, **63**, (5), pp. 3261–3270
- [11] Li, S.H., Liu, Z.G.: ‘Adaptive speed control for permanent magnet synchronous motor system with variations of load inertia’, *IEEE Trans. Ind. Electron.*, 2009, **56**, (8), pp. 3050–3059
- [12] Chen, Z., Huang, J.: ‘Stabilization and regulation of nonlinear systems: a robust and adaptive approach’ (Springer, London, 2015)
- [13] Shieh, H.J., Hsu, C.H.: ‘An adaptive approximator-based backstepping control approach for piezoactuator-driven stages’, *IEEE Trans. Ind. Electron.*, 2008, **55**, (4), pp. 1729–1738
- [14] Morawiec, M.: ‘The adaptive backstepping control of permanent magnet synchronous motor supplied by current source inverter’, *IEEE Trans. Ind. Inf.*, 2013, **8**, (2), pp. 1047–1055
- [15] Kim, K.S., Park, Y., Oh, S.H.: ‘Designing robust sliding hyperplanes for parametric uncertain systems: a Riccati approach’, *Automatica*, 2000, **36**, (7), pp. 1041–1048
- [16] Tong, S., Sui, S., Li, Y.: ‘Fuzzy adaptive output feedback control of mimo nonlinear systems with partial tracking errors constrained’, *IEEE Trans. Fuzzy Syst.*, 2015, **4**, (23), pp. 729–742
- [17] Choi, H.H.: ‘LMI-based sliding surface design for integral sliding model control of mismatched uncertain systems’, *IEEE Trans. Autom. Control*, 2007, **52**, (4), pp. 736–742
- [18] Yang, J., Li, S.H., Yu, X.: ‘Sliding-mode control for systems with mismatched uncertainties via a disturbance observer’, *IEEE Trans. Ind. Electron.*, 2013, **60**, (1), pp. 160–169
- [19] Yang, J., Chen, W.H., Li, S.H.: ‘Non-linear disturbance observer-based robust control for systems with mismatched disturbances/uncertainties’, *IET Control Theory Appl.*, 2011, **5**, (18), pp. 2053–2062

- [20] Back, J., Shim, H.: ‘An inner-loop controller guaranteeing robust transient performance for uncertain MIMO nonlinear system’, *IEEE Trans. Autom. Control*, 2009, **54**, (7), pp. 1601–1607
- [21] Han, J.: ‘From PID to active disturbance rejection control’, *IEEE Trans. Ind. Electron.*, 2009, **56**, (3), pp. 900–906
- [22] Zheng, Q., Dong, L., Lee, D.H., et al.: ‘Active disturbance rejection control for mems gyroscopes’. Proc. of American Control Conf., 2008, pp. 4425–4430
- [23] She, J.H., Xin, X., Pan, Y.D.: ‘Equivalent-input-disturbance approach-analysis and application to disturbance rejection in dual-stage feed drive control system’, *IEEE Trans. Mechatronics*, 2011, **16**, (2), pp. 330–340
- [24] Yang, Z., Tsubakihara, H., Kanae, S., et al.: ‘A novel robust nonlinear motion controller with disturbance observer’, *IEEE Trans. Control Syst. Technol.*, 2008, **16**, (1), pp. 137–147
- [25] Li, S.H., Yang, J.: ‘Robust autopilot design for bank-to-turn missiles using disturbance observers’, *IEEE Trans. Aerosp. Electron. Syst.*, 2013, **1**, (49), pp. 558–579
- [26] Li, S.H., Yang, J., Chen, W.H., et al.: ‘*Disturbance observer-based control: methods and applications*’ (CRC Press, 2014)
- [27] Yang, J., Zolotas, A., Chen, W.H., et al.: ‘Robust control of nonlinear MAGLEV suspension system with mismatched uncertainties via DOBC approach’, *ISA Trans.*, 2011, **50**, (3), pp. 389–396
- [28] Liu, H.X., Li, S.H.: ‘Speed control for PMSM servo system using predictive functional control and extended state observer’, *IEEE Trans. Ind. Electron.*, 2012, **59**, (2), pp. 1171–1183
- [29] Wang, J.X., Li, S.H., Yang, J., et al.: ‘Extended state observer-based sliding mode control for PWM-based DC-DC buck power converter systems with mismatched disturbances’, *IET Control Theory Appl.*, 2015, **9**, (4), pp. 579–586
- [30] Becedas, J., Trapero, J.R., Mamani, G., et al.: ‘A fast on-line algebraic estimation of a single-link flexible arm applied to gpi control’. IEEE Industrial Electronics, IECON 2006 – 32nd Annual Conf. on, 2006, pp. 85–90
- [31] Levant, A.: ‘Higher-order sliding modes’, differentiation and outputfeedback control’, *Int. J. Control.*, 2003, **76**, (9/10), pp. 924–941
- [32] Ding, S.H., Levant, A., Li, S.H.: ‘Simple homogeneous sliding-mode controller’, *Automatica*, 2016, **67**, pp. 22–32
- [33] Liu, J.X., Laghrouche, S., Waek, M.: ‘Observer-based higher order sliding mode control of power factor in three-phase ac/dc converter for hybrid electric vehicle applications’, *Int. J. Control.*, 2014, **87**, (6), pp. 1117–1130
- [34] Huang, Y., Xue, W.C.: ‘Active disturbance rejection control: methodology and theoretical analysis’, *ISA Trans.*, 2014, **53**, (4), pp. 963–976
- [35] Yang, J., Su, J.Y., Li, S.H., et al.: ‘High-order mismatched disturbance compensation for motion control systems via a continuous dynamic sliding-mode approach’, *IEEE Trans. Ind. Inform.*, 2014, **10**, (1), pp. 604–614
- [36] Khalil, H.K.: ‘*Nonlinear systems*’ (Prentice-Hall, 1996, 2nd edn.)
- [37] Li, S., Tian, Y.P.: ‘Finite-time stability of cascaded time-varying systems’, *Int. J. Control.*, 2007, **80**, (4), pp. 646–657
- [38] Duran, M.J., Prieto, J., Barrero, F.: ‘Space vector PWM with reduced common-code voltage for five-phase induction motor drives operating in overmodulation zone’, *IEEE Trans. Power Electron.*, 2013, **28**, (8), pp. 4030–4040
- [39] Mattavelli, P.: ‘An improved deadbeat control for UPS using disturbance observer’, *IEEE Trans. Ind. Electron.*, 2005, **52**, (1), pp. 206–211
- [40] Ertl, H., Kolar, J.W., Zach, F.C.: ‘A novel multicell DC-AC converter for applications in renewable energy systems’, *IEEE Trans. Ind. Electron.*, 2002, **49**, (5), pp. 1048–1057
- [41] Zheng, W., Li, S.H., Wang, J.X., et al.: ‘Sliding-mode control for three-phase PWM inverter via harmonic disturbance observer’. Proc. of the 34th Control Conf., July 2015, pp. 7988–7993
- [42] Wang, Y.G., Wang, D.W., Zhou, K.L., et al.: ‘Modelling and robust repetitive control of PWM DC/AC converters’. IEEE Int. Symp. on Intelligent Control, 2007, pp. 214–219